

# The EMIR Observing Program Manager System : Science Simulator

Johan Richard<sup>a</sup>, Roser Pelló<sup>a</sup>, Thierry Contini<sup>a</sup>, Sylvie Brau-Nogué<sup>b</sup> and Christian Lucuix<sup>b</sup>

<sup>a</sup>Laboratoire d'Astrophysique de Toulouse-Tarbes, 14 avenue Edouard Belin, 31400 Toulouse, France;

<sup>b</sup>Laboratoire d'Astrophysique de Toulouse-Tarbes, 57 avenue d'Azereix, BP 826 65008 Tarbes Cedex, France;

## ABSTRACT

We present in this poster paper the Science Simulation aspects of the EMIR Observing Program Manager System (EOPMS). EMIR is a multi-slit near-IR spectrograph presently under development for the Gran Telescopio de Canarias (GTC). We present the scientific functionalities of the EOPMS and its ability to provide the user with the required information during the different observing phases. The Exposure Time Calculator (ETC) and the Image Simulator (IS) are described in details, focusing on some unique capabilities with respect to the presently available tools, such as the possibility of 2D spectra simulation and realistic 1D extraction.

**Keywords:** Near-IR spectrographs, Observing Tools, ETC, Science Simulation

## 1. INTRODUCTION : EOPMS - OVERVIEW

We present in this poster paper the Science Simulation aspects of the EMIR<sup>1</sup> Observing Program Manager System (hereafter EOPMS). EMIR is a multi-slit near-IR spectrograph presently under development for the Gran Telescopio de Canarias (GranTeCan, hereafter GTC). Versatile simulation tools such as the EOPMS are specially needed for the next generation of near-IR ground-based spectrographs, to allow detailed feasibility studies on increasingly complex science projects.

The EOPMS under development was designed to fulfill three main purposes closely related to science exploitation:

- During the development phase, this tool is needed to test the different configurations and to quantify precisely the instrumental effects resulting from technical or scientific choices. It allows to control the efficiency of the whole system and its ability to fulfil the scientific requirements. These are important points in the definition of survey programs such as the Cosmos/GOYA project (see for example Balcells et al. 2003<sup>2</sup>).
- As a kernel tool for future observers using EMIR. During Phase I preparation, it will be required as a general purpose exposure time calculator, including image simulation capabilities.
- During Phase II, the EOPMS will be used for a detailed preparation of observation sequences, and to optimize the choice of the targets to be included in masks before performing Multi-slit configurations.

The EOPMS includes the following functionalities:

- The Exposure Time Calculator (ETC).
- The Image Simulator (IS) for the production of realistic synthetic 1D and 2D spectra.

---

Further author information: (Send correspondence to J.R.)

J.R.: E-mail: jrichard@ast.obs-mip.fr, Telephone: +33 (0)5 61 33 28 24

R.P.: E-mail: roser@obs-mip.fr, Telephone: +33 (0)5 61 33 28 12

- The Multi-slit Positioner (MSP).
- A user interphase allowing to prepare observation sequences according to GTC standards.

This poster paper is only focused on the science simulation aspects of the EOPMS. The plan of the paper is as follows. In Section 2.1 we present the science simulation scheme. The ingredients included in the simulator are described as well as the use of the different parameters. Section 3 illustrates the functionalities of this tool with examples of use. Further improvements are given in Section 4.

## 2. EOPMS SCIENCE SIMULATIONS

### 2.1. Simulation scheme

In order to reproduce realistic observations, the EOPMS has to include a detailed simulation for each of the following elements, with a wide range of input parameters :

#### 2.1.1. Simulation of Individual Sources

The basic properties to define for an individual source are:

- The source is assumed to be located in the center of the slit.
- The object morphology: point sources or extended objects. In the case of extended objects, the user can choose between a constant surface brightness and an exponential profile (specified by a core radius). In an extended version of the EOPMS, other brightness profiles (e.g. de Vaucouleurs profile) will be implemented.
- The Spectral Energy Distribution of the source (SED). This is done by selecting a template spectrum from the available libraries :

Object type	Reference template	Resolution	Wavelength coverage
Stars	Pickles <sup>3</sup>	~500	1150-25000 Å
Galaxies :			
-Empirical Templates	Coleman et al. 1980 <sup>4</sup>	~125	1000-10000Å (**)
-Empirical Starbursts	Kinney et al. 1996 <sup>5</sup>	~370-500	1200-10000Å (**)
-Synthetic evolutionary models(*)	Bruzual & Charlot 2003 <sup>6</sup>	~2000 at 3200-9500 Å ~40-500 otherwise	97Å - 9.7μm
-Synthetic Starbursts(*)	Starburst99 <sup>7</sup>	variable	90-25000Å
Quasars	Hatziminaoglou et al. 2000 <sup>8</sup>	variable	90-25000Å

**Table 1.** Templates libraries included in the EOPMS; (\*) indicates that the implementation is planned.(\*\*) Extended with Buruzual & Charlot templates between 97Å and 9.7 μm.

In the case of quasars, we use a library of synthetic spectra following the prescriptions by Hatziminaoglou et al. 2000,<sup>8</sup> but spanning a wider parameter space. Predictions for galaxies based on synthetic spectra will be possible in an upgraded version through standard evolutionary codes and models (such as the Bruzual & Charlot 2003<sup>6</sup> code based on STELIB,<sup>9</sup> or Starburst99<sup>7</sup>).

User templates, either empirical or theoretical, can be used as input SEDs.

The user can add any fiducial emission lines to the template spectrum, and select for each of them values for the central wavelength, Full-Width Half-Maximum (FWHM) and integrated flux. Only gaussian profiles have been implemented at the present stage. In an advanced version of the EOPMS the user will have the choice between other types of profile (lorentzian, ...).

- The redshift : defined as  $z = \Delta\lambda/\lambda = (\lambda(measured) - \lambda(restframe))/\lambda(restframe)$  is the cosmological shift in the wavelength frame.

- The integrated magnitude for point sources, or central surface brightness for extended objects, in a specified filter band and photometric system (Vega, AB system, ...). Magnitudes are either apparent or absolute, in which case the user shall specify the cosmological parameters to be used for the calculations.

The magnitude or surface brightness is used as a scaling of the selected SED, including Lyman-forest in the computation, following the Madau et al. 1995<sup>10</sup> prescription.

- Possible internal reddening, produced inside the source itself by dust extinction, is simulated by a dust-screen model. The user can choose both the extinction value and the reddening law among the following possibilities :
  1. Seaton et al. 1979<sup>11</sup> fit by Fitzpatrick et al. 1986<sup>12</sup> for the Milky Way
  2. Prévot et al. 1984<sup>13</sup> and Bouchet et al. 1985<sup>14</sup> for the Small Magellanic Cloud (SMC)
  3. Calzetti et al. 2000<sup>15</sup> for starburst galaxies

### 2.1.2. Simulation of Multi-Object modes

The EOPMS will include the possibility of multiple objects image simulation, as a tool to prepare the design of Multi-Objects masks.

The 2D distribution of target sources on the field is taken either from a pre-existing catalogue (real observations or simulations), or from an input image. It contains the input parameters for sources, or a set of specifications to generate a pure synthetic field, magnitude or flux limited. The EOPMS shall be able to process in principle any input catalogue given by the user, and containing the following information:

- The position of each object in the field, and the astrometric accuracy. Positions are given in Right Ascension and Declination (absolute astrometry), or in relative (x, y) values in arcsecs with respect to a source in the field with known astrometry.
- Integrated magnitudes or central surface brightness in a specified filter band and photometric system.
- The object morphology, specified by the brightness profile and ellipticity. When this information is not known, a general profile is used (point source or exponential).
- Redshift and SED, as for individual sources, in case of simulated catalogues.

In the final version, the EOPMS shall propose a tutorial display on a limited number of random simulated fields according to a given set of parameters: magnitude-limited blank-fields, clusters of galaxies or stars. This mode is to be used for training using the MSP.

## 2.2. Sky background simulation

A model for the sky is included in the simulations, given the important role of sky subtraction errors in near-infrared photometry and spectroscopy. It includes a detailed model for the OH airglow lines, which dominate between 1 and 2.3 microns, as well as known telluric absorptions features. OH airglow lines are simulated through Gaussian profiles. We used in this model our knowledge of the sky in Canary Islands when available, completed by observations from ESO when necessary (e.g. for the OH lines, Rousselot et al. 2000<sup>16</sup> ). The model also includes the sky background thermal emission.

## 2.3. Observational Conditions simulation

The EMIR Simulator should be able to take into account a variation in the standard pre-selected observational conditions:

- Seeing.
- Atmospheric refraction (as a function of the air-mass, temperature, pressure ...).

- A detailed model for sky emission and absorption, including its variation as a function of the air-mass and other relevant parameters.
- The presence of dust. Dust absorption is introduced in terms of magnitudes in a given filter band.
- The object position accuracy (with respect to the slit or with respect to the central pixel in the imaging mode) and the acquisition stability.

#### 2.4. Optics simulation

The EOPMS simulates the GTC + EMIR optics transmission as a function of wavelength and position on the field. At first order, only wavelength is important, and the object is assumed to be located on the center of the field. The advanced version should take into account possible vignetting effects, the presence of scattered light, possible geometrical distortions and the PSF across the field.

#### 2.5. Thermal Emission simulation

The EOPMS includes the thermal emission from the telescope and surrounding area, as well as the emission from the spectrograph itself. This is done at first through a rough measurement of the emissivity, using the known data from other existing telescopes and IR instruments. The final version shall include the specific template for EMIR thermal emission.

#### 2.6. Instrumental Configuration simulation

The EOPMS introduces the precise instrumental configuration in the calculations. This means:

- transmission through the different filters and dispersive elements, as obtained from experimental measurements,
- spectral resolution corresponding to the wavelength range selected by the user,
- slit configuration (width, length and profile),
- total exposure and individual readout times.

#### 2.7. Detector simulation

The EOPMS introduces the precise detector parameters, as obtained from the most recent experimental measurements :

- Pixel scale : the angular resolution on the sky of an image element.
- Gain : the number of electrons per Activity Detector Unit (ADU)
- Detection Quantum Efficiency (DQE). This value depends on the position on the detector (x,y) and the wavelength.
- Dark current : as measured in  $e - /sec$ .
- Readout mode : the EOPMS includes differences between the readout modes in the detector parameters.
- Readout noise. It is simulated through gaussian noise.
- Photon noise. It is simulated through Poisson noise.
- Saturation level : this level corresponds to the maximum number of counts registered by a pixel. The typical value in infrared detectors is 60000 e-. Non-linearity effects should be introduced at the level required according to measurements on the EMIR science detector.

Cosmetic effects should be considered as additional ingredients if needed after the complete characterization of the EMIR science detector.

## 2.8. Synopsis of the overall simulation

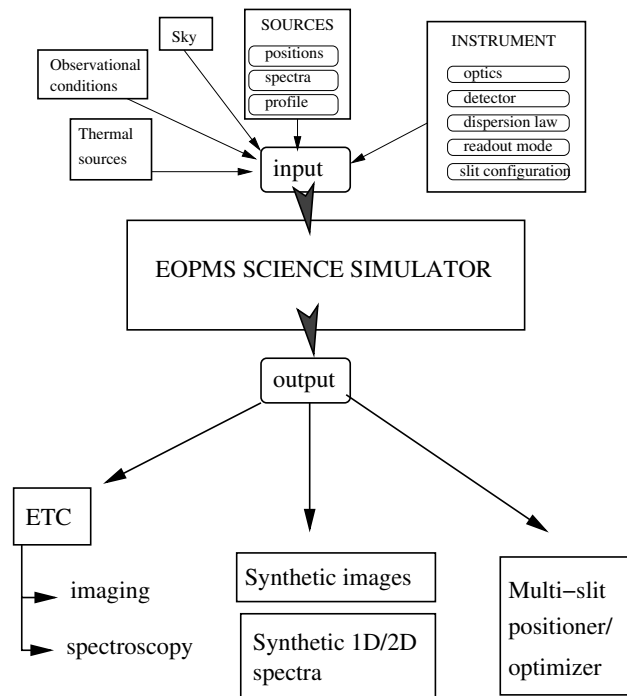


Figure 1. Overview of the EOPMS. The main input and output parameters are presented.

## 3. ETC - IS : FUNCTIONALITIES AND EXAMPLES OF USE

The EOPMS will be used as an observing tool during Phase I and Phase II. The user will specify a set of input parameters (including detailed source properties, observational conditions and instrumental configuration) and the output mode (image and/or table files).

### 3.1. Exposure Time Calculator

#### 3.1.1. Summary of main output results

The ETC provides the following output data for both Imaging and Spectroscopy Modes:

- The Signal to Noise Ratio (S/N) expected as a function of exposure time.
- The exposure time needed to reach a given S/N.

In the Imaging Mode, the S/N can refer to:

- the central pixel of the object,
- the mean value in case of extended sources (specified through a surface brightness value),
- a circular aperture of fixed size (seeing size or an arbitrary value), or
- an isophotal aperture.

In the Spectroscopic Mode, the S/N can refer to:

- S/N per pixel or per resolved wavelength interval.
- Averaged S/N within a given wavelength region.

These output data shall be released as an XML VOTable, easily edited and displayed for visualisation purposes. The Signal to Noise ratio (SNR) is defined as:

$$S/N = \frac{\Phi_o t}{\sqrt{(\Phi_o + \Phi_s) t + T_e t + ron^2}} \quad (1)$$

where  $\Phi_o$  and  $\Phi_s$  are respectively the source and sky fluxes, in terms of photons per second and pixel (or in photons  $sec^{-1} \text{\AA}^{-1} pixel^{-1}$  or photons  $sec^{-1} Hz^{-1} pixel^{-1}$ , when computing the S/N as a function of the wavelength).  $T_e$  is the dark current (in  $e^- sec^{-1} pixel^{-1}$ ),  $ron$  is the read-out noise (in  $e^- pixel^{-1}$ ), and  $t$  is the exposure time. The fluxes are defined as:

$$\Phi(\lambda) = F_0(\lambda)A(\lambda)T(\lambda)Q(\lambda) \times S \times pixel^2 \quad (2)$$

where  $F_0(\lambda)$  is the flux at the top of the Earth's atmosphere,  $A(\lambda)$  is the atmospheric transmission,  $T(\lambda)$  is the filter bandpass,  $Q(\lambda)$  is the total system throughput (telescope, spectrograph and detector DQE), and  $S$  is effective collecting area.

This expression is adapted to compute different S/N estimates, depending on the ETC modes.

### 3.1.2. ETC Example

Figure 2 illustrates the use of the ETC. An Irregular (Im type) galaxy template is used to derive the evolution of the S/N ratio in the extracted spectrum as a function of Exposure Time. The final spectrum is obtained by the composition of individual spectra of 900 sec exposure time.

## 3.2. Image Simulator

### 3.2.1. Summary of main output results

From the input parameters specified by the user, this mode creates 3 outputs :

- Extracted 1D spectra, containing the following information:
  - wavelength,
  - object flux at the top of the Earth's atmosphere,
  - object flux as seen through the EMIR configuration (in ADU/pixel or  $e^-/pixel$ ),
  - mean sky flux (in ADU/pixel or  $e^-/pixel$ ), as computed through a realistic extraction procedure,
  - total flux, sum of the contributions for the object and sky fluxes (in ADU/pixel or  $e^-/pixel$ ),
  - extracted spectrum (total - mean sky flux) (same units),
  - S/N ratio as a function of wavelength.
- raw 2D image obtained through a slit of specified length, width and geometry, and
- sky-subtracted 2D image.

Images are released in FITS format.

In order to keep the best possible S/N on the final 1D spectra, the object is extracted across the slit through the usual procedure, i.e. each pixel along the spatial direction is weighted according to its S/N. In practice, to obtain the S/N ratio as a function of wavelength we compute for each spectral element in the extracted spectrum the equivalent quantity:

$$S/N = \frac{\Phi(object + sky) - \Phi(sky)}{\sqrt{\Phi(object + sky)}} \quad (3)$$

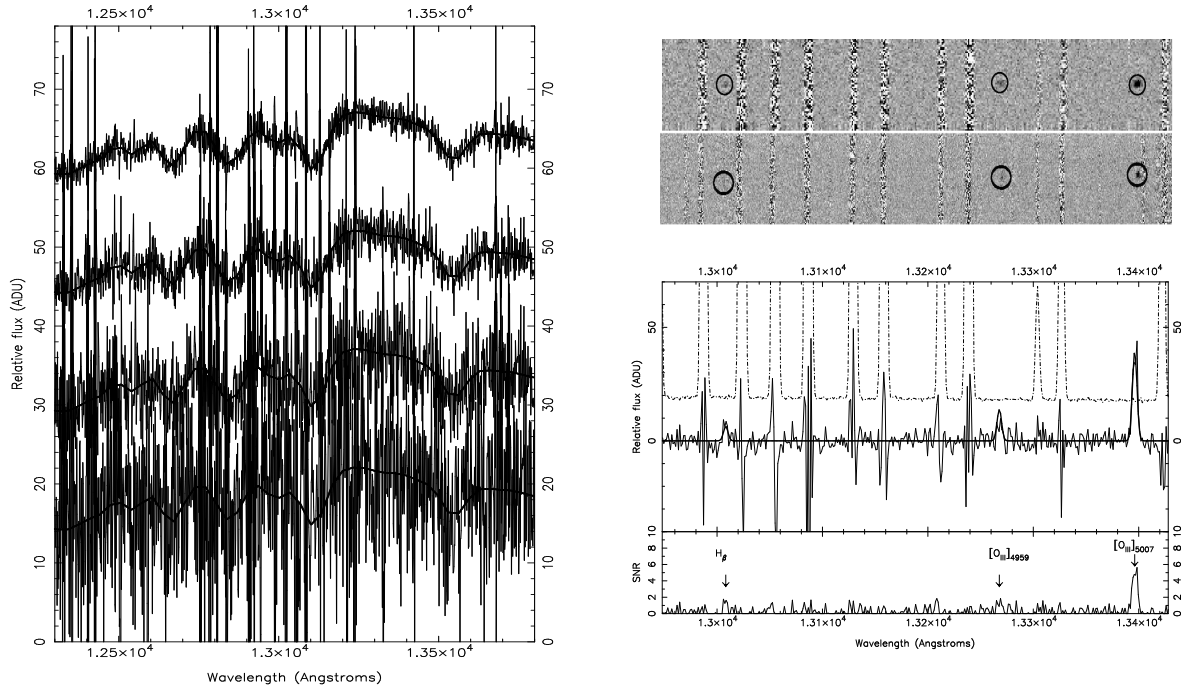


**Figure 2. Example of simulation results.**

*Left part* : ETC output for an Irregular (Im type) galaxy, showing the evolution of the extracted spectrum as a function of magnitude, for a given Exposure Time. The galaxy template is scaled to an apparent magnitude ranging between  $J=17$  and  $20$  from top to bottom, and the exposure time used is  $3600$  ksec. All spectra are shifted one to another by a constant vertical value for clarity.

*Right part* : IS output for a  $z=1.676$  galaxy dominated by its emission lines. From top to bottom : simulated 2D spectrum, observed 2D spectrum with VLT/ISAAC (see Richard et al. 2003<sup>17</sup>), sky model spectrum (dash-dotted line), object model spectrum (bold line) and sky-subtracted observed object spectrum, Observed Signal to Noise ratio as a function of wavelength with detected emission lines.

### 3.2.2. IS Example

Figure 2 illustrates the behaviour of the IS. We have used the IS to reproduce the observed 2D spectrum of a  $z=1.676$  galaxy recently observed with VLT/ISAAC (see Richard et al. 2003<sup>17</sup>). This object is dominated by its emission lines, a situation which could be easily simulated with our EOPMS. The 2D simulated spectrum is much more useful for feasibility studies than a simple measurement of the S/N ratio.

## 4. FURTHER IMPROVEMENTS

In an advanced version of the EOPMS, we foresee several improvements leading to a more realistic simulation of the instrument and site behaviour :

- Detailed information concerning to the instrument transmission, detector characteristics, thermal environment and sky features will be updated during and after commissioning.
- The EOPMS will include a modelling of the moonlight contamination (in emission) as a function of the moon phase, the moon-target separation and relative positions, and the moon and target altitude, for a mean value of the local extinction (see Krisciunas & Schaefer 1991<sup>18</sup> and Simons et al. 1993<sup>19</sup>).
- When simulating a long acquisition procedure (long exposure in Spectroscopic Mode or shift-and-stack procedure in Imaging Mode), a variation mode in the OH emission will be introduced in this advanced version. This variation is observed in a few minutes period of time (Ramsay et al. 1992<sup>20</sup>). The absorption

and emission sky conditions vary as a function of the observation period and the position of the target field on the sky. Such variations are not included in present day simulation tools.

## ACKNOWLEDGMENTS

We are grateful to J.-F. Le Borgne and other colleagues at LA2T, Instituto de Astrofísica de Canarias and Gran Telescopio Canarias for useful comments and discussions on this project.

## REFERENCES

1. F. Garzon, S. Barrera, S. Correa, J. Diaz-Garcia, A. Fragoso-Lopez, F. Fuentes, F. Gago, J.-C. Lopez-Ruiz, A. Manescau, J. Patron, J. Perez-Espinos, V. S. de la Rosa, A. Villegas, and P. Redondo, “EMIR : the GTC NIR multiobject imager-spectrograph,” *Proceedings of the SPIE Instrument Design and Performance for Optical/Infrared Ground-based Telescopes*. **4841**, pp. 1539–1547, 2003.
2. M. Balcells, “EMIR science prospects,” in *Revista Mexicana de Astronomia y Astrofisica Conference Series*, pp. 69–72, 2003.
3. A. J. Pickles, “A Stellar Spectral Flux Library: 1150-25000 Å,” *PASP* **110**, pp. 863–878, July 1998.
4. D. Coleman, C. Wu, and D. Weedman, “Colors and magnitudes predicted for high redshift galaxies,” *ApJS*. **43**, pp. 393–416, 1980.
5. A. L. Kinney, D. Calzetti, R. Bohlin, K. McQuade, T. Storchi-Bergmann, and H. Schmitt, “Template ultraviolet to near-infrared spectra of star-forming galaxies and their application to k-corrections,” *ApJ* **467**, p. 38, 1996.
6. G. Bruzual and S. Charlot, “Stellar population synthesis at the resolution of 2003,” *MNRAS* **344**, pp. 1000–1028, Oct. 2003.
7. C. Leitherer, D. Schaerer, J. Goldader, R. Delgado, C. Robert, D. Kune, D. de Mello, D. Devost, and T. Heckman, “Starburst99: Synthesis models for galaxies with active star formation,” *ApJS* **123**, pp. 3–40, 1999.
8. E. Hatziminaoglou, G. Mathez, and R. Pelló, “Quasar candidate multicolor selection technique: a different approach,” *A&A* **359**, pp. 9–17, July 2000.
9. J.-F. Le Borgne, G. Bruzual, R. Pelló, A. Lançon, B. Rocca-Volmerange, B. Sanahuja, D. Schaerer, C. Soubiran, and R. Vílchez-Gómez, “STELIB: A library of stellar spectra at  $R \sim 2000$ ,” *A&A* **402**, pp. 433–442, May 2003.
10. P. Madau, “Radiative transfer in a clumpy universe: The colors of high-redshift galaxies,” *ApJ* **441**, pp. 18–27, 1995.
11. M. J. Seaton, “Interstellar extinction in the UV,” *MNRAS* **187**, pp. 73P–76P, June 1979.
12. E. L. Fitzpatrick and D. Massa, “An analysis on the shapes of ultraviolet extinction curves. I - The 2175 Å bump,” *ApJ* **307**, pp. 286–294, Aug. 1986.
13. M. L. Prevot, J. Lequeux, L. Prevot, E. Maurice, and B. Rocca-Volmerange, “The typical interstellar extinction in the Small Magellanic Cloud,” *A&A* **132**, pp. 389–392, Mar. 1984.
14. P. Bouchet, J. Lequeux, E. Maurice, L. Prevot, and M. L. Prevot-Burnichon, “The visible and infrared extinction law and the gas-to-dust ratio in the Small Magellanic Cloud,” *A&A* **149**, pp. 330–336, Aug. 1985.
15. D. Calzetti, L. Armus, R. Bohlin, A. Kinney, J. Koornneef, T. Storchi-Bergmann, and et al., “The dust content and opacity of actively star-forming galaxies,” *ApJ* **533**, pp. 682–695, 2000.
16. P. Rousselot, C. Lidman, J. Cuby, G. Moreels, and G. Monnet, “Night-sky spectral atlas of OH emission lines in the near-infrared,” *A&A* **354**, pp. 1134–1150, 2000.
17. J. Richard, D. Schaerer, R. Pelló, J.-F. Le Borgne, and J.-P. Kneib, “Discovery of a faint R-band drop-out: A strongly reddened lensed star forming galaxy at  $z = 1.68$ ,” *A&A* **412**, pp. L57–L60, Dec. 2003.
18. K. Krisciunas and B. Schaefer, “A model of the brightness of moonlight,” *Astronomical Society of the Pacific, Publications* **103**, pp. 1033–1039, 1991.



19. D. A. Simons, C. C. Clark, J. M. Kerr, S. Massey, S. S. Smith, and D. W. Toomey, “Canada-France-Hawaii telescope near-infrared camera project,” in *Proc. SPIE Vol. 1946, p. 502-512, Infrared Detectors and Instrumentation*, Albert M. Fowler; Ed., pp. 502–512, Oct. 1993.
20. S. Ramsay, C. Mountain, and T. Geballe, “Non-thermal emission in the atmosphere above mauna kea,” *MNRAS* **259**, pp. 751–760, 1992.